ACADEMIA ROMÂNĂ
Revue Roumaine de Chimie
https://www.icf.ro/rrch/

Rev. Roum. Chim.,
2026, *71*(3–4), 265–274
DOI: 10.33224/rrch.2026.71.3-4.10

MOLECULAR STRUCTURE AND MÖSSBAUER SPECTROSCOPY OF THE ORGANIC-INORGANIC HYBRID SALT: *BIS*[1,1'-METHYLENEDIPYRIDINIUM] HEXACYANOFERRATE(II) OCTAHYDRATE

Mahmoud M. Al-KTAIFANI, [*a] Mohammad K. SABRA[b] and Waël S. AL-KHOURY[c]

[a]Department of Radioisotopes, Atomic Energy Commission, P.O. Box 6091, Damascus, Syrian Arab Republic
[b]Department of Physics, Atomic Energy Commission, P.O. Box 6091, Damascus, Syrian Arab Republic
[c]Department of Chemistry, Atomic Energy Commission, P.O. Box 6091, Damascus, Syrian Arab Republic

Received October 21, 2025

The molecular structure of $(C_{11}H_{12}N_2)_2[Fe(CN)_6]\cdot 8H_2O$ is confirmed by powder X-ray diffraction study as well as the Mössbauer spectroscopy investigation was carried out. The molecular structure exhibits the two distinctive organic dications $(C_{11}H_{12}N_2)^{2+}$, inorganic anion $[Fe(CN)_6]^{4-}$, and eight uncoordinated H_2O molecules occupying channels in the crystal lattice. The Fe(II) center of $[Fe(CN)_6]^{4-}$ adopts an ideal octahedral geometry and is coordinated by six C atoms of CN ligands. Hirshfeld surface analysis is also performed to visualize the non-covalent interactions that stabilized the crystal structure of the complex. The Mössbauer spectrum of the complex was acquired at room temperature. The absence of quadrupole splitting ($\Delta Q=0$) is observed, referring to a highly symmetric electric field gradient at the iron center, which is consistent with a symmetrical octahedral coordination geometry of the $[Fe(CN)_6]^{4-}$ ion. The obtained isomer shift (δ) is larger than its corresponding one for the structurally related $K_4[Fe(CN)_6]\cdot 3H_2O$. This noticeable difference of Mössbauer spectra for $(C_{11}H_{12}N_2)_2[Fe(CN)_6]\cdot 8H_2O$ and $K_4[Fe(CN)_6]\cdot 3H_2O$ is clearly due to different chemical, electrical and steric effects generated by the dication $(C_{11}H_{12}N_2)^{2+}$ compared to cation K^+ at the environment of the iron nucleus.

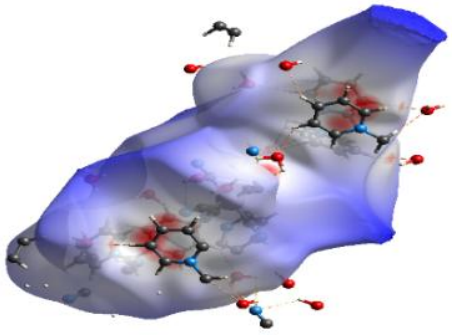

INTRODUCTION

There is a considerable interest in designing new complexes to support groups in various research fields. Organic-inorganic hybrid salts are currently inquired as novel materials in different research areas; such as materials science, crystal engineering, magnetic and optical applications.[1–4] In the last past years, ferrocyanides; in particular; Prussian blue $Fe_4[Fe(CN)_6]_3$ and its analogues have attracted ongoing interest due to their distinctive magnetic, spectroscopic, redox and structural properties.[5–7] Potassium ferrocyanide $K_4[Fe(CN)_6]\cdot 3H_2O$ is a diamagnetic compound, because its central Fe^{2+} has all its electrons paired in the *d* orbitals due to the strong field of the cyanide ligands, featuring low-spin (Fe(II) (t_{2g}^6, S=0) in octahedral coordination. Its Mössbauer spectra show a sharp singlet (IS ≈ –0.15 to –0.3

* Corresponding author: cscientific@aec.org.sy

mm/s, QS ≈ 0) due to high symmetry.[8,9] The mentioned characteristics; make ferrocyanides-potentially attractive materials in electronic research such as solar energy conversion and electro-chromic devices.[5] In the last years, the organic dication 1,1′-methylenedipyridinium $(C_{11}H_{12}N_2)^{2+}$ was utilized by us to prepare some different organic-inorganic hybrid ionic complexes of the form; $(C_{11}H_{12}N_2)[MCl_4]$, (M = Zn,[10] Cd,[10] Cu,[11] Pt[12]), $(C_{11}H_{12}N_2)[AuCl_4]_2$,[11] $(C_{11}H_{12}N_2)[PtCl_6]$,[12] $(C_{11}H_{12}N_2)[Cu(NO_3)_4]$[13] and $(C_{11}H_{12}N_2)[Fe(CN)_5NO]\cdot 5H_2O$.[14,15] Furthermore, the optical nonlinearity and Mössbauer spectrum of $(C_{11}H_{12}N_2)[Fe(CN)_5NO]\cdot 5H_2O$ were also investigated.[14,15] Previously, the synthesis, spectroscopic characterization and the optical nonlinearity investigation of the $(C_{11}H_{12}N_2)_2[Fe(CN)_6]\cdot 8H_2O$ were also reported by us.[16] As a continuation of our studies, in this article, we introduce the crystal, molecular structure of the complex $(C_{11}H_{12}N_2)_2[Fe(CN)_6]\cdot 8H_2O$ determined through powder X-ray diffraction and Mössbauer spectroscopy analysis.

RESULTS AND DISCUSSION

Synthesis, spectroscopic identification and optical-non-linear investigation of the $(C_{11}H_{12}N_2)_2[Fe(CN)_6]\cdot 8H_2O$ (Fig. 1) were previously reported.[16] As expected, the FTIR and ^1H and $^{13}C\{^1H\}$ NMR spectra for the complex; each has the same feature to their corresponding ones of the recently published related organic–inorganic hybrid salts $[C_{11}H_{12}N_2][MCl_4]$ (M = Zn,[10] Cd,[10] Cu,[11] Pt[12]) and the parent molecule $(C_{11}H_{12}N_2)Cl_2$, except the extra peak associated with cyanide group. It was of interest to complete the characterization of the complex by studying the molecular structure and Mossbauer spectroscopy analysis for $(C_{11}H_{12}N_2)_2[Fe(CN)_6]\cdot 8H_2O$.

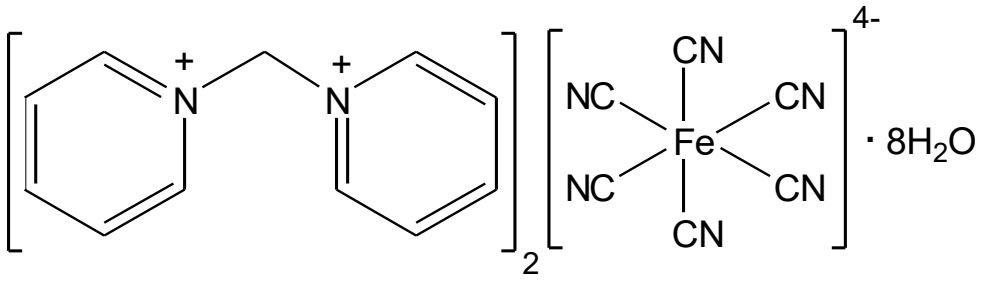

Fig. 1 – Molecular structure of $(C_{11}H_{12}N_2)_2[Fe(CN)_6]\cdot 8H_2O$.[16]

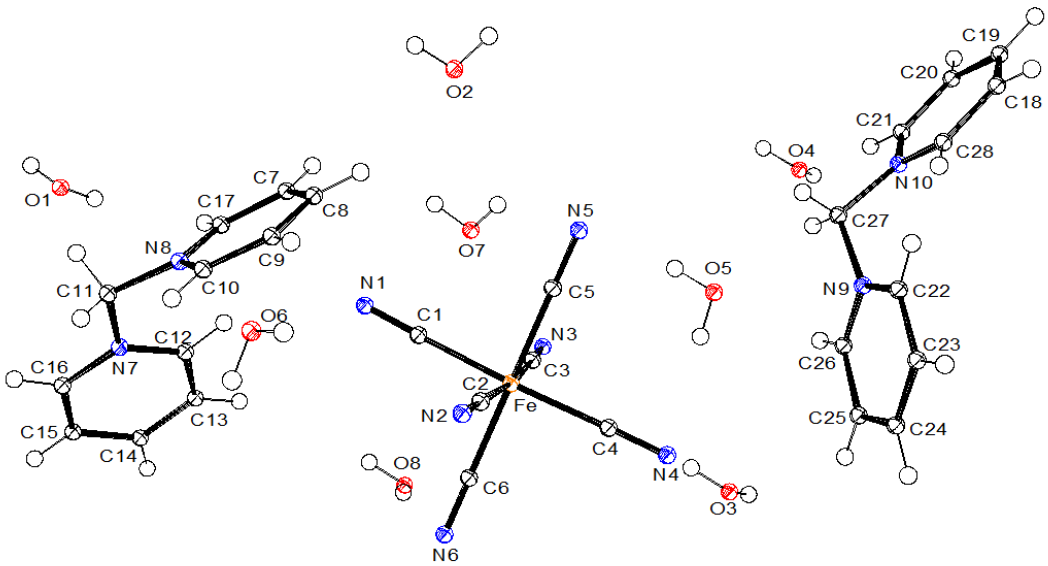

Fig. 2 – The asymmetric unit of crystal structure of $(C_{11}H_{12}N_2)_2[Fe\ (CN)_6]\cdot 8H_2O$ shows the atomic numbering. Displacement ellipsoids are drawn at the 50% probability level. H atoms are represented as small spheres of arbitrary radii.

Although many attempts were carried out to crystalize the complex, no-good quality crystals were formed. Therefore, the crystal and molecular structures are determined by powder X-ray diffraction study. The powder X-ray investigation reveals that the structure of the complex is ionic consisting of two distinctive independent organic dications $(C_{11}H_{12}N_2)^{2+}$, inorganic anion $[Fe(CN)_6]^{4-}$, and eight uncoordinated H_2O molecules (Fig. 2).

The Fe(II) center of $[Fe(CN)_6]^{4-}$ has almost an ideal octahedral geometry and is coordinated by six C centers of CN ligands. The Fe–C bond distances lie in the range 1.92(2)–1.94(7) Å with average Fe–C bond distance of 1.93(6) Å (see Table 1). The obtained bond distances are in their expected ranges, and in agreement with their corresponding ones in the structurally related complexes $(C_{18}H_{18}N_2)_2[Fe(CN)_6] \cdot 4H_2O$, where $((C_{18}H_{18}N_2)^{2+}$ is 1,1'-[1,4-Phenylenebis(methylene)]dipyridinium) and $(NH_4)(C_8H_{20}N)_2[Fe(CN)_6] \cdot 3H_2O$, where $((C_8H_{20}N)^+$ is tetraethylammonium).[17,18] The Fe–C–N bond angles are almost linear with only very minor deviation from linearity (the largest Fe–C–N angle is 179.47° and the smallest angle is 178.45°) with average C-N bond length of 1.15(2) Å. Both of them lie in their normal ranges and they are comparable to their counterparts in the related complexes $(C_{18}H_{18}N_2)_2[Fe(CN)_6] \cdot 4H_2O$ and $(NH_4)(C_8H_{20}N)_2$ - $[Fe(CN_6] \cdot 3H_2O$.[17,18]

Table 1

Selected bond lengths (Å) and angles (°) for $(C_{11}H_{12}N_2)_2[Fe(CN)_6] \cdot 8H_2O$

Bond	Bond length (Å)	Angle	Bond angle (°)
Fe—C1	1.93(8)	C1—Fe—C2	91.3(1)
Fe—C2	1.94(5)	Cl—Fe—C3	84.0(1)
Fe—C3	1.94(7)	C1—Fe—C4	172.8(8)
Fe—C4	1.93(6)	C1—Fe—C5	89.3(5)
Fe—C5	1.92(7)	C1—Fe—C6	91.2(3)
Fe —C6	1.92(2)	C2—Fe—C3	174.9(3)
C1—N1	1.15(2)	C2—Fe—C4	95.6(7)
C2—N2	1.15(2)	C2—Fe—C5	89.7(1)
C3—N3	1.15(3)	C2—Fe—C6	87.3(3)
C4—N4	1.15(3)	C3—Fe—C4	90.0 (6)
C5—N5	1.15(1)	C3—Fe—C5	88.4(6)
C6— N6	1.15(2)	C3—Fe—C6	94.6(6)
		C4—Fe—C5	89.2(6)
		C4—Fe—C6	90.5(3)
		C5—Fe—C6	176.9(5)

In the crystal packing of the complex, eight uncoordinated H_2O molecules occupy the channels within the crystal lattice. The water molecules are involved in hydrogen bonding with cyanide groups and among each other (C–N· · ·H–O and O–H· · · O–H). Moreover, weak intermolecular C–H· · ·O and C–H· · ·N contacts are observed. These standard and nonstandard hydrogen bonds are linking dictions $(C_{11}H_{12}N_2)^{2+}$, anions $[Fe(CN)_6]^{4-}$ and H_2O molecules to form three dimensional network structure (Fig. 3). These hydrogen bonds are likely very effective in the stabilization of the crystal packing of the complex (Table 2).

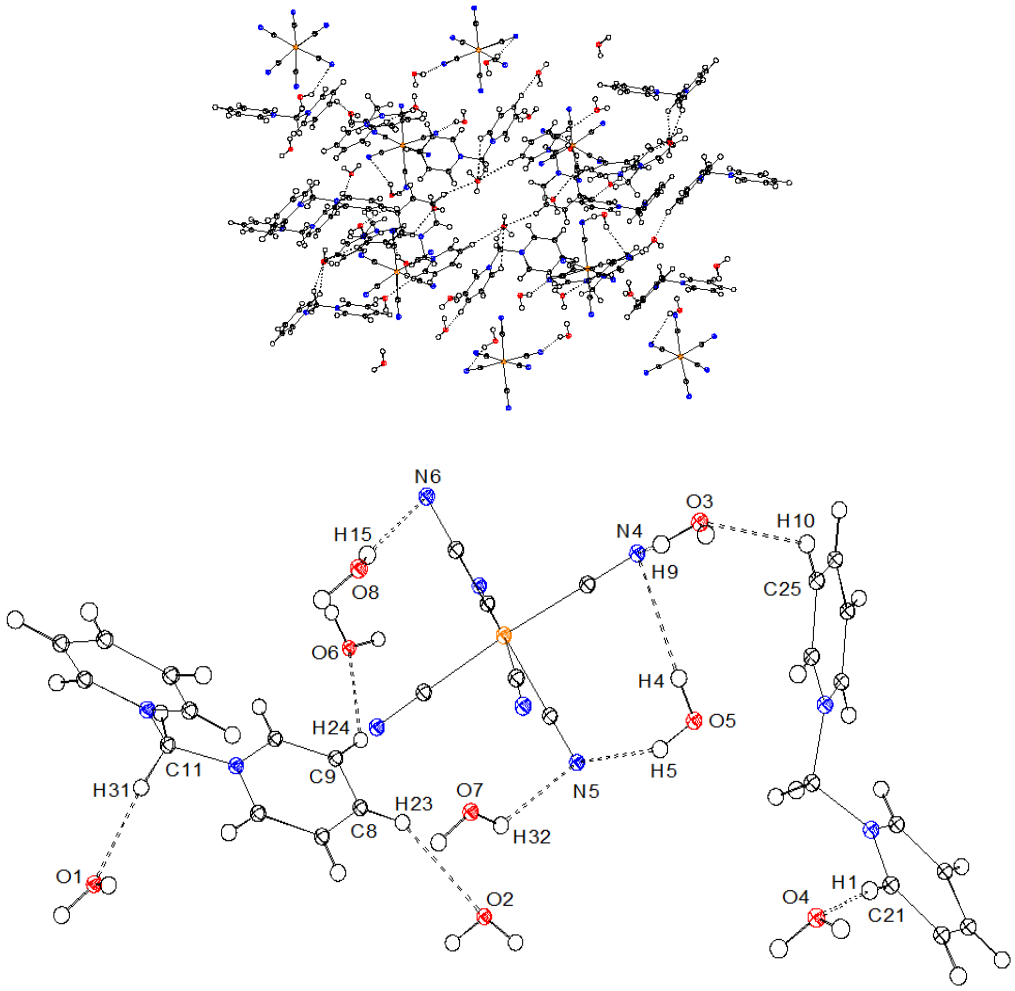

Fig. 3 – Portion of the packing diagram in the unit cell (above) and asymmetric unit (bellow) of $(C_{11}H_{12}N_2)_2[Fe(CN)_6]\cdot 8H_2O$. Dashed lines indicate hydrogen bonds between water molecules, $[Fe(CN)_6]^{4-}$, and $(C_{11}H_{12}N_2)^{2+}$.

Table 2

Hydrogen bond distances (Å) and bond angles (°) for the complex.

	d(D–H)	***d(H···A)***	***d(D···A)***	***Angle(D–H···A)***
O3–H9···N4	0.851	2.044	2.583	120.56
O5–H4···N4	0.850	2.521	3.287	150.48
O5–H5···N5	0.851	2.613	3.185	125.65
O7–H32···N5	0.851	2.478	3.137	134.84
O8–H15···N6	0.849	2.492	3.298	158.78
C8–H23···O2	0.951	2.523	3.387	149.05
C9–H24···O6	0.950	2.478	3.207	133.46
C11–H31···O1	0.991	2.278	3.115	141.50
C21–H1···O4	0.949	2.346	3.293	174.71
C25–H10···O3	0.950	2.413	3.114	130.44

Symmetry code: (i) *x*, *y*, *z*; (ii) -*x*, *y*+1/2, - *z*+1; (iii) -*x*, −*y*, - *x*, (iv) *x*,−*y*+1/2, *z*+1/2.

To visualize the intermolecular interactions of $(C_{11}H_{12}N_2)_2[Fe(CN)_6]\cdot 8H_2O$ that stabilize the crystal structure of the complex, Hirshfeld surface analysis and 2D-fingerprint plots were carried on the Cif file using the Crystal Explorer package.[19] The Hirshfeld surface is shown in Fig. 4 through the descriptor d_{norm}. The normalized contact distance (d_{norm}) is essentially based on both contact distances between nearest atoms present inside (d_i) and outside (d_e) the surface, respectively. The red spots are attributed to O–H···N, O–H···O, C–H···O. In addition, it is noticeably from the Hirshfeld surface the C···C (π … π) stacking interactions in the surface mapped of individual pyridine ring with other adjacent pyridine ring in the unit cell.

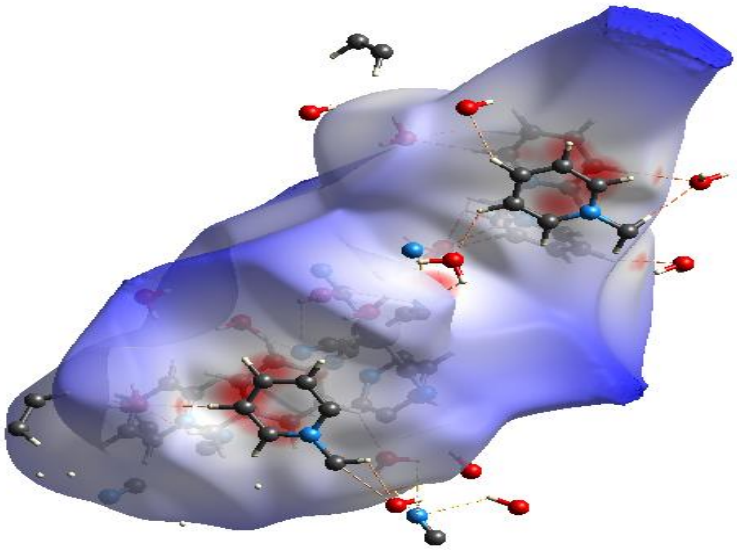

Fig. 4 – Hirshfeld surfaces mapped for d_{norm} surfaces of $(C_{11}H_{12}N_2)_2[Fe(CN)_6]\cdot 8H_2O$.

The d_{norm} surface can be resolved into 2D fingerprint plots (Fig. 5), which analyses all intermolecular contacts and gives a quantitatively summary of the type and strength of intermolecular contacts experienced by the $(C_{11}H_{12}N_2)^{2+}$ and $[Fe(CN)_6]^{4-}$ and H_2O molecules in the crystal. Figure 5 highlights particular atom pair contacts. The H···H contacts (61.7%) are the most encountered interactions in the title complex due to the abundance of hydrogen atoms on the molecular surface but with no important role in the stabilization of structure. The N···H and O···H interactions contribute 9.3% and 4.3% respectively to the total Hirshfeld surface, which indicate also important roles in stabilization of the crystal packing. The C···H and C···C (π…π) interactions contribute 3.2% and 1.8% respectively to the total Hirshfeld surface, both have the smallest contribution on the Hirshfeld surface.

The Mössbauer spectrum was fitted to a sum of Lorentzians using WinNormos[20–22] that uses nonlinear optimization with least-squares statistics (a χ^2-method). Mössbauer Spectra of potassium ferrocyanide $K_4[Fe(CN)_6]\cdot 3H_2O$ (Low-Spin, S=0) and $(C_{11}H_{12}N_2)_2[Fe(CN)_6]\cdot 8H_2O$ samples at room temperature (10.3±0.3 °C, in the winter) are shown in Fig. 6. In this figure, most of the potassium ferrocyanide have a well-resolved symmetric singlet due to symmetrical (spherical) charge distribution at ^{57}Fe nucleus. The asymmetry that can be caused by the Goldanskii-Karyagin effect (GKE)[23] or oriented texture in the absorber was not observed.

As can be shown in the Fig. 6, no quadrupole splitting (ΔQ=0) is observed for both $K_4[Fe(CN)_6]\cdot 3H_2O$ and $(C_{11}H_{12}N_2)_2[Fe(CN)_6]\cdot 8H_2O$ referring to the highly symmetric electric field gradient at the iron center, consistent with the symmetrical octahedral coordination geometry of the $[Fe(CN)_6]^{4-}$ ion. As expected, their isomer shifts (δ) equal to –0.181±0.002 and –0.174±0.001 $mm\cdot s^{-1}$ (r.t. α-Fe) respectively, with line widths (Γ) equal to 0.306±0.005 and 0.342±0.004 $mm\cdot s^{-1}$ and χ^2= 0.962 and 0.936 at room temperature respectively (Table 3). The isomer shift value, indicates the presence of Fe(II).[24] It is also noticeable that the |δ| for $(C_{11}H_{12}N_2)_2[Fe(CN)_6]\cdot 8H_2O$ is relatively larger than its idem for $K_4[Fe(CN)_6]$- $\cdot 3H_2O$, while its line width less than its corresponding for $K_4[Fe(CN)_6]\cdot 3H_2O$.[20] This is readily due to the presence of 1,1′-methylenedipyridinium dications and eight

H_2O molecules, which generates a distinct electrical and chemical environment at the iron nucleus in $(C_{11}H_{12}N_2)_2[Fe(CN)_6]\cdot 8H_2O$ compared to the environment at the iron center produced by cations K^+ and three H_2O molecules in $K_4[Fe(CN)_6]\cdot 3H_2O$.

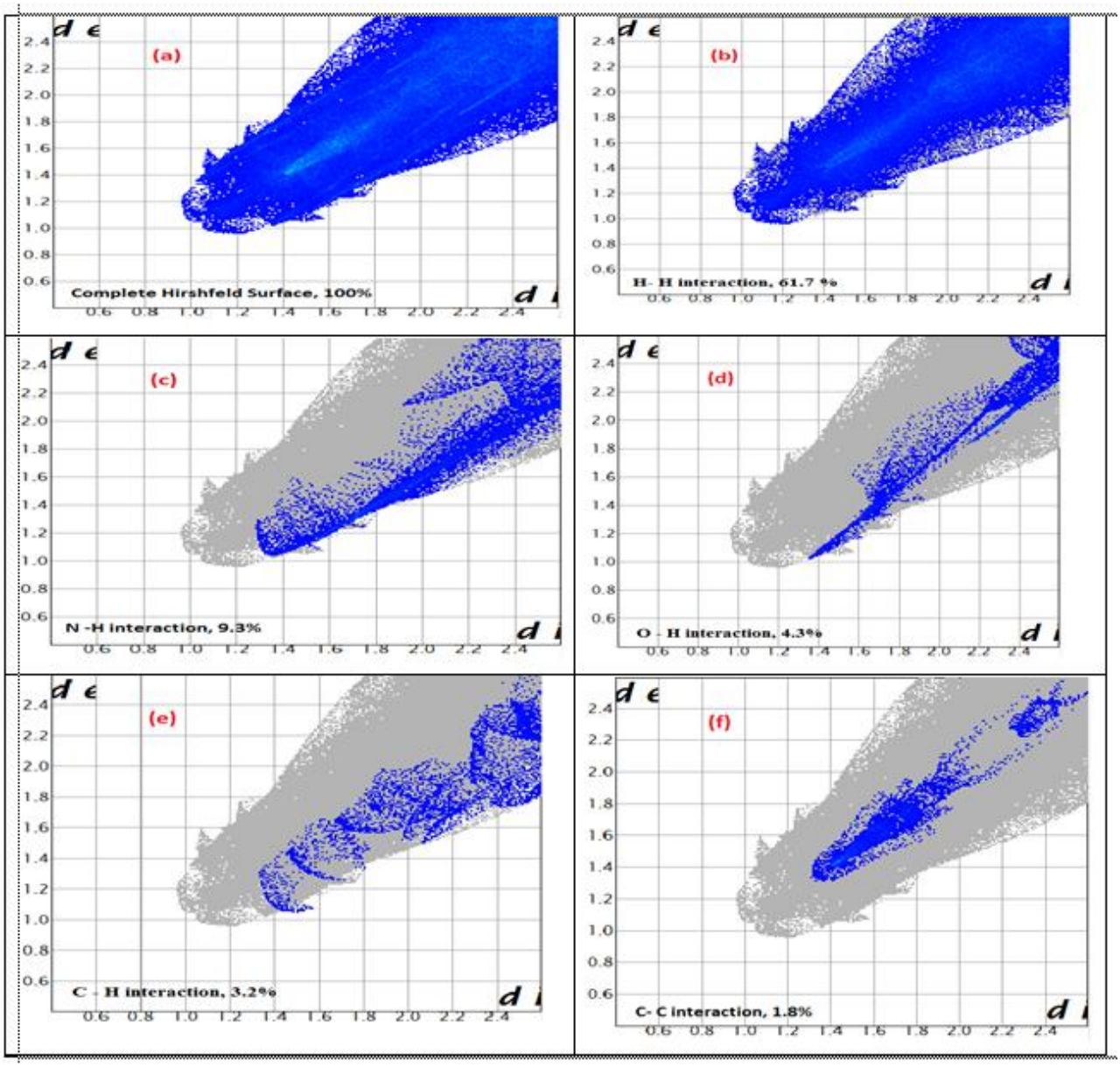

Fig. 5 – **(a–f)** The two-dimensional fingerprint plots showing: **a)** – complete Hirshfeld surface; **b)** – H···H interactions; **c)** – N···H interactions; **d)** – O···H interactions; **e)** – C···H interactions; **f)** – C···C(π…π) interactions.

Table 3

Mössbauer parameters for the $K_4[Fe(CN)_6]\cdot 3H_2O$ and $(C_{11}H_{12}N_2)_2[Fe(CN)_6]\cdot 8H_2O$

Material	δ [mm·s^{-1}]	Γ [mm·s^{-1}]	χ^2
$K_4[Fe(CN)_6]\cdot 3H_2O$	–0.181±0.002	0.306±0.005	96.23%
$(C_{11}H_{12}N_2)_2[Fe(CN)_6]\cdot 8H_2O$	–0.174±0.001	0.342±0.004	93.60%

Isomer shift values respect to α-Fe at room temperature.

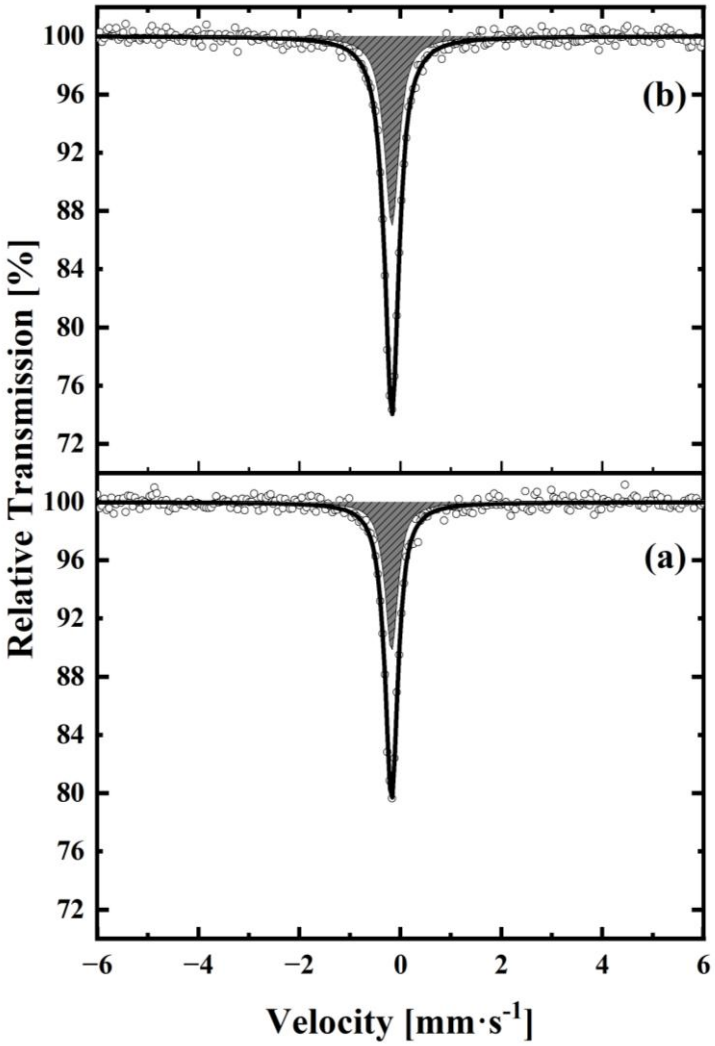

Fig. 6 – Mössbauer spectra and their fits using one singlet for: a) – $K_4[Fe(CN)_6]\cdot 3H_2O$; b) – $(C_{11}H_{12}N_2)_2[Fe(CN)_6]\cdot 8H_2O$ at room temperature.

EXPERIMENTAL

Reactions and manipulations were carried out in air with reagent grade solvents. $(C_{11}H_{12}N_2)_2[Fe(CN)_6]\cdot 8H_2O$ was prepared according to literature method.[16] Briefly, A solution of $(C_{11}H_{12}N_2)Cl_2\cdot H_2O$ (0.522 g, 1.99 mmol) in H_2O (4 ml) was added to a solution of $K_4[Fe(CN)_6]\cdot 3H_2O$ (0.404 g,0.96 mmol) in H_2O (4 ml) at room temperature and stirred for an hour. The mixture was then left aside for two days to give red powder, which was separated, washed with Et_2O and dried to afford a red brick powder (426 mg, yield 63%).

Microanalysis was performed using *EURO EA* (Italy). The characterization data of the complex are summarized in Table 4. Powder X-ray diffraction was performed on a *Stoe Transmission diffractometer* (Stadi P) (Stoe & CIE, Germany). Mössbauer spectrum was collected with a constant acceleration transmission mode setup, with a ∼100 mCi $^{57}Co/Rh$ gamma-ray source (April 2017, Ritverc Co.), and was obtained with a spectrometer equipped with a Mössbauer Velocity transducer (WissEl GmbH model MA-260S) controlled by a linear function driving (WissEl GmbH Mössbauer Drive Unit model MR-360). Value of Mössbauer isomer shift is quoted relatively to α-Fe foil (30 μm, Ritverc Co.). The Mössbauer spectrum is fitted to a sum of Lorentzians by means of a least-squares procedure using software package WinNormos for Igor (written by R. A. Brand, at Laboratorium für Angewandte Physik, Universität Duisburg, D-47048, Duisburg-Germany). All Mössbauer measurements were achieved at room temperature.

Table 4

Basic characterization data for $(C_{11}H_{12}N_2)_2[Fe(CN)_6]\cdot 8H_2O$

Formula	***Molecular Weight***	***Elemental analysis***			***Yield***	***M.p.***
		C	*H*	*N*	*%*	*°C*
$C_{28}H_{40}FeN_{10}O_8$	*700.53*	w_i*(calc.)/% 48.01* w_i*(found)/% 47.43*	*5.75* *5.59*	*19.99* *20.35*	*63*	*192* *(dec)*

Crystal structure determination for $(C_{11}H_{12}N_2)_2Fe(CN)_6]\cdot 8H_2O$ by powder X-ray diffraction

The crystal structure was determined using the powder X-ray diffraction data which is collected using the transmission diffractometer (*STADI-P STOE*, Darmstadt, Germany), with Cu K_α radiation (λ= 1.54059 Å) and a germanium monochromator operated at 50 kV and 30 mA. The scanning angle starts at 5° and ends at 100° with a scanning rate of 1° per minute.

In order to solve the material structure, the first attempt to find the crystal structure is performed with the help of Monte Carlo and grid search (McMaille program), which is implemented in *the EXPO2014* software.[25] A monoclinic cell with a satisfactory weighted profile R-factor (R_{wp}= 0.036) is found. Where the structure belongs to the space group $P21/c$. The found crystal parameters are a = 17.459 (3) Å, b = 16.783 (14) Å, c = 24.612 (5) Å, β =107.457°. The structure is further refined using Rietveld method as implemented in *GSAS-II* package[26] and the figure of merit [M (20) =24.5] becomes better. The final values of the crystallographic data and refinement goodness factors are shown in Table 5. Where we can see the weighted profile R-factor (R_{wp} = 0.033) is improved. The final Rietveld plots of the X-ray diffraction patterns are given in Fig. 7 and the 2θ axis is cut at 55° where no significance peaks are existed after this value.

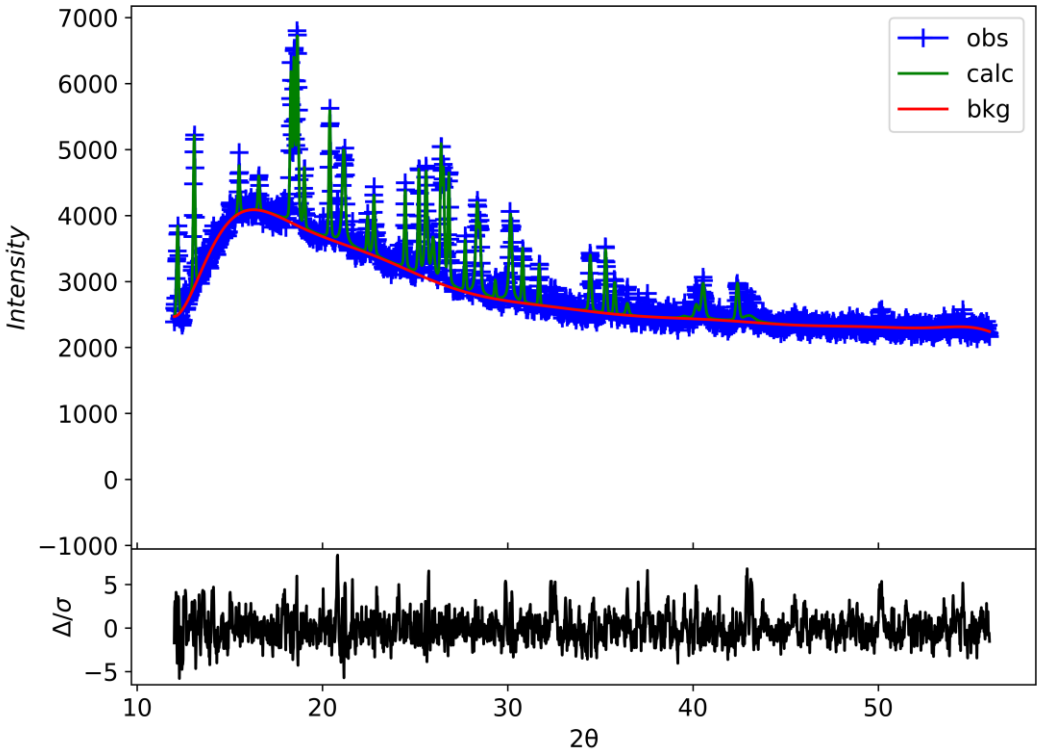

Fig. 7 – The final Rietveld pattern for $(C_{11}H_{12}N_2)_2[Fe(CN)_6]\cdot 8H_2O$. The (+) is the observed values and (–) are the fitted ones. The black line is the difference between the observed and the fitted values.

Table 5

Crystallographic data and refinement parameters for $(C_{11}H_{12}N_2)_2[Fe(CN)_6]\cdot 8H_2O$

CCDC number	2472388
Chemical formula	$C_{28}H_{40}FeN_{10}O_8$
M_r	700.54
Crystal system, space group	Monoclinic, $P2_1/c$
Temperature (K)	300
a, b, c (Å)	17.459 (3), 16.7828 (14), 24.612 (5)
β (°)	107.457 (7)
V (Å^3)	6879.6 (16)
Z	4
Radiation type	$K\alpha_{1,2}$, λ = λ, =, 1.54051,, 1.54433, Å Å
μ (mm^{-1})	1.96
Specimen shape, size (mm)	Cylinder, 15 × 5
Data collection	
Diffractometer	STOE transmission STADI-P
Specimen mounting	Powder loaded between two Mylar foils
Data collection mode	Transmission
Scan method	Step
2θ values (°)	$2\theta_{min}$ = 5.24 $2\theta_{max}$ = 90.22 $2\theta_{step}$ = 0.02
Refinement	
R factors and goodness of fit	R_p = 0.023, R_{wp} = 0.033, R_{exp} = 0.018, $R(F^2)$ = 0.00000, χ^2 = 3.269
No. of data points	4250
No. of parameters	31

CONCLUSION

The molecular structure, Hirshfeld surface analysis and Mössbauer spectroscopy of the organic-inorganic ionic complex $(C_{11}H_{12}N_2)_2[Fe(CN)_6]\cdot 8H_2O$ are investigated. The molecular structure shows the two distinctive organic dications $(C_{11}H_{12}N_2)^{2+}$, tetraanion $[Fe(CN)_6]^{4-}$, and eight uncoordinated water molecules. The H_2O molecules are occupying channels linking the dications $(C_{11}H_{12}N_2)^{2+}$ and anions $[Fe(CN)_6]^{4-}$ in the crystal lattice to form three dimensional network. The Mössbauer spectrum of the complex gives the expected singlet with no quadruple splitting and different isomer shift (δ) comparing to the parent salt $K_4[Fe(CN)_6]\cdot 3H_2O$.

Supplementary information. CCDC 2472388 contains the supplementary crystallographic data for this paper. This data can be obtained free of charge via www.ccdc.cam.ac.uk/conts/retrieving.html (or from the Cambridge Crystallographic Data Centre, 12, Union Road, Cambridge CB2 1EZ, UK; fax: +44 1223 336033).

Acknowledgements. The authors would like to acknowledge the great support of the Director General of the AECS for his support throughout this research.

The authors would like, also, to thank the Heads of Radioisotopes and physics Departments for their help. Thanks are extended to Mr. Abd A. Alsharif, Mrs. K. Latifi, Miss Fatemh Maksoud and Mr. Tareq Jeejan for their help in conducting the laboratory experiments and measurements.

REFERENCES

1. S. H. Mir, L. A. Nagahara, T. Thundat, P. Mokarian-Tabari, H. Furukawa and A. Khosla, *J. Electrochem. Soc.*, **2018**, *165*, B3137–B3156.
2. N. Kimizuka and T. Kunitake, *Adv. Mater,* **1996**, *8*, 89–91.
3. D. B. Mitzi, M. T. Prikas and K. Chondroudis, *Chem. Mater,* **1999**, *11*, 542–544.
4. F. Bonhomme and M. G. Kanatzidis, *Chem. Mater*, **1998**, *10*, 1153–1159.
5. P. V. Bernhardt, F. Bozoglián, B. P. Macpherson and M. Martınez, *Coord. Chem. Rev.,* **2005**, *249*, 1902–1916,
6. K. R. Dunbar and R. A. Heintz, *Prog. Inorg. Chem*., **1997**, *45*, 283–391.
7. M. Ohba, and H. Okawa, *Coord. Chem. Rev*., **2000**. *198*, 313–328.
8. A. L. Kholmetskii, T. Yarman and O. V. Missevitch, *Physica Scripta*, **2008**, *77*, 035302, doi: 10.1088/0031-8949/77/03/035302.
9. L. Daniel Reger, J. Derek Elgin, E. A. Foly, M. D. Smith, F. Grandjean and G. J. Long, *Inorg. Chem.*, **2009**, *48*, 9393-9401. doi: 10.1021/ic901259e.
10. M. M. Al-Ktaifani and M. K. Rukiah, *Chem. Pap.*, **2011**, *65*, 469–476.
11. M. M. Al-Ktaifani and M. K. Rukiah, *Acta Cryst.,* **2012**, *C68*, m246–m250.
12. M. M. Al-Ktaifani and M. K. Rukiah, *Chem. Pap*., **2012**, *66*, 1032–1038. doi:10.2478/s11696-012-0221-8.
13. M. M. Al-Ktaifani and M. K. Sabra, *Rev. Roum. Chim.* **2019**, *64*, 469–477.
14. M. D. Zidan, M. M. Al-Ktaifani and A. Allahham, *Acta Phys. Polonica A*, **2016**, *130*, 1326–1331. doi:10.12693/APhysPolA.130.1326.
15. M. M. Al-ktaifani, M. K. Sabra and W. S. AL-Khoury, *Rev. Roum. Chim.* **2025**, *70*, 717–723. doi: 10.33224/rrch.2025.70.9-10.15.
16. M. D. Zidan, M. M. Al-Ktaifani and A. Allahhama, Optik, **2015**, *126*, 1491–1494.
17. M.-S. Tang, Y.-J. Wu, X.-C. Liu, C.-X. Du and Y.-Y. Niu*, Acta Cryst.,* **2007**. *E63*, m2517.
18. M. M. MalĬarová, J. Černák and W. Massa, Acta Cryst., **2007**, *C63*, m187–m189.
19. P. R. Spackman, M. J. Turner, J. J. McKinnon, S. K. Wolff, D. J. Grimwood, D. Jayatilaka and M. A. Spackman, *J. Appl. Cryst.*, **2021**, 54, 10061011.
20. R. A. Brand, J. Lauer and D. M. Herlach, *J. Phys. F Met. Phys.*, **1983**, *13*, 675–683.
21. R. A. Brand, *Nuclear Instruments and Methods in Physics Research*, **1987**, *B28*, 398–416.
22. R. A. Brand and G. Le Caër, *Nuclear Instruments and Methods in Physics Research*, **1988**, *B34*, 272–284.
23. H. –D. Pfannes and U. Gonser, *Appl. Phys*., **1973**, *1*, 93–102.
24. P. Gütlich, R. Link, A. Trautwein, Mössbauer Spectroscopy and Transition Metal Chemistry, Springer, Berlin 2011.
25. A. Altomare, C. Cuocci, C. Giacovazzo, A. Moliterni, R. Rizzi, N. Corriero and A. Falcicchio, *J. Appl. Cryst.*, **2013**, *46*, 1231–1235.
26. B. H. Toby and R. B. Von Dreele, *J. Appl. Cryst*., **2013**, *46*, 544–549.